Full Paper

Synthesis, Thermal Behavior and Energy Performance of Nitroguanidyl-Functionalized Energetic Materials

Jiachao Bai,[a] Ergang Yao,[b] Libai Xiao,[b] Jie Zhou,[a] Yinghui Ren,*[a] Fengqi Zhao,[b] and Wenzhong Shen[c]

Abstract: Six nitroguanidyl-functionalized nitrogen-rich compounds were synthesized and characterized by EA, FT-IR, and NMR. In addition, the crystal structures of ANPTz, CABNG, and FANG were further determined by X-ray single-crystal diffractometer. The thermal decomposition behaviours were studied by the DSC-TG-FTIR-MS coupling technique and the results showed that all the compounds had good thermal stability, among which ANPTz had the best thermal stability ($T_d = 211.03\,°C$). Also, HCN, CO_2, H_2O, and NO_2 were released during thermal decomposition process. The self-accelerating decomposition temperature (T_{SADT})

and thermal explosion critical temperature (T_b) were calculated to evaluate thermal safety, and the relative order was as follows: FANG ($T_{SADT} = 198.68\,°C$, $T_b = 209.97\,°C$) > ANPTz ($T_{SADT} = 194.12\,°C$, $T_b = 208.63\,°C$) > BANTz ($T_{SADT} = 182.52\,°C$, $T_b = 207.54\,°C$) > AANG ($T_{SADT} = 180.04\,°C$, $T_b = 188.35\,°C$) > CABNG ($T_{SADT} = 176.80\,°C$, $T_b = 187.32\,°C$) > MABNG ($T_{SADT} = 173.61\,°C$, $T_b = 184.29\,°C$). The results indicated that FANG had the acceptable sensitivity ($IS = 7.84$ J), good detonation performance ($D = 8551$ m·s^{-1}, $P = 32.33$ GPa), and the significant catalytic effect (the decomposition temperature of RDX decreased by $8.31\,°C$).

Keywords: nitroguanidyl-functionalized · thermal behavior · energy performance

1 Introduction

High energy density materials (HEDMs) or high energy density compounds (HEDC) have become the focus of attention in the field of energetic materials since they were proposed [1–6]. For the design and synthesis of HEDMs, the current focus is on achieving a balance between energy (density, detonation velocity, detonation pressure, and heat of formation) and safety (impact sensitivity, friction sensitivity, electrostatic discharge sensitivity). Therefore, considerable efforts have been made to develop novel HEDMs with comprehensive properties including high density, positive heat of formation, excellent detonation performance, good thermal stability, and low sensitivity. Although a large number of HEDMs have been designed and synthesized [7–9], disappointingly, they do not satisfy the balance of the above relations. In short, HEDMs with superior comprehensive performance (energy and sensitivity are well balanced) are one of the future development directions in the field of energetic materials.

For HEDMs, one of the effective synthetic methods is to introduce some high-energy groups such as nitro, azido, azo, or nitroimino into the framework structure of high nitrogen molecules (chain-like structure or ring-like structure). Nitroguanidine, as a commonly used non-sensitive energetic monomer, is widely used in propellants, propellants power, and low-damage explosives because of its superior detonation performance [10, 11]. Therefore, it is a good solution to modify nitroguanidine properly and introduce it into the framework structure of high-nitrogen molecules. For instance, because of the chemical reactivity of amino

groups, -NO_2 groups can be introduced into nitroguanidine to improve its detonation performance. The nitration product DNG (1,2-dinitroguanidine) contains two nitro groups, which are acidic and tend to react with alkaline substances because of the electron absorption effect. The detonation performance of ADNG, generated by the reaction with ammonium carbonate, is equivalent to that of RDX [12]. Fischer, Klapötke and Stierstorfer [13] reacted nitroguanidine with 80% hydrazine hydrated to obtain ANQ (amino-nitroguanidine) with 58.8% nitrogen content, $\rho = 1.722$ g·cm^{-3}, $D = 8729$ m·s^{-1}, $P = 30.7$ GPa, and low sensitivity. Since the presence of amino and hydrazine increases the reactivity of ANQ, many researchers have synthesized its derivatives with good properties [14–16]. Zhang, He, Yin, and Shreeve

[a] *J. Bai, J. Zhou, Y. Ren*
School of Chemical Engineering
Xi'an Key Laboratory of Special Energy Materials
Northwest University
Xi'an 710069, P.R. China
*e-mail: renyinghui_ren@163.com
[b] *E. Yao, L. Xiao, F. Zhao*
Science and Technology on Combustion and Explosion Laboratory
Xi'an Modern Chemistry Research Institute
Xi'an 710065, P.R. China
[c] *W. Shen*
State Key Laboratory of Coal Conversion
Institute of Coal Chemistry
Chinese Academy of Sciences
Taiyuan 030001, P.R. China

[17] used water as the reaction solvent to react N-methyl-N-nitroso-N′-nitroguanidine (MMNG) with heterocyclic compounds (triazine and tetrazine). Under relatively mild conditions, high energy insensitive nitroguanidine groups were successfully introduced into the skeleton of high nitrogen heterocycles, and the synthesized compound was characterized with high nitrogen content, symmetrical structure, and high stability (the molecule contains heterocycles). Similarly, a series of furazan-functionalized 5-nitroimino-1,2,4-triazoles were obtained using condensation of readily and commercially available MNNG with furazan-functionalized carboxylic acid hydrazides [18]. The process was straightforward, high yielding, highly efficient, scalable, and the obtained compounds have high measured density, high heat of formation, excellent detonation velocity, and detonation pressure.

Based on the above mentioned, six energetic compounds were designed by introducing the high-energy nitroguanidine groups into the skeletons of 1,2,4,5-tetrazine ring, and chain hydrazide. The structures have been fully characterized, and the thermal decomposition behavior and mechanism have been studied by DSC-TG-FTIR-MS coupling technique. Also, the effects on the thermal decomposition of RDX are discussed.

2 Experimental Section

2.1 Materials and Instruments

All chemicals purchased from Aladdin Biochemical Technology Company, Shanghai, China, were commercially available reagents of analytical grade and used without further purification. RDX is provided by Xi'an modern chemistry research institute.

Elemental analysis was performed on a Vario EL-III element analyzer. Fourier transfer infrared spectrometry (FT-IR) was determined on an Equinox55 spectrometer with a KBr presser bit. ^{1}H and ^{13}C NMR spectra were recorded on 400 MHz and 100 MHz (INOVA-400) nuclear magnetic resonance operating at 400 MHz and 100 MHz, respectively, by using DMSO-d_6 as the solvent. ^{14}N NMR spectra were recorded on Bruker-AV500 instrument in DMSO-d_6 at 25 °C. The thermal behaviors of the samples were determined using differential scanning calorimetry (DSC, Q2000, TA, USA.) and simultaneous thermal analysis (SDT, Q600, TA, USA) in N$_2$ atmosphere. Impact sensitivity (IS) was measured according to the UN Recommendations on the Transport of Dangerous Goods, Manual of Tests, and Criteria.

The single-crystal data were recorded by a Bruker SMART APEX II X-ray diffractometer that used M-$K\alpha$ radiation ($\lambda = 0.071073$ nm) and a graphite monochromator. Using OLEX2 [19], the crystal structures were solved by direct methods and refined by full-matrix least-squares on F^2 with SHELXL-2014 [20].

2.2 Synthesis and Characterization

Six nitroguanidyl-functionalized nitrogen-rich compounds were named 3-(aminonitroguanidino)-6-(3,5-dimethylpyrazole)-1,2,4,5-tetrazine (ANPTz), 3,6-bis(aminonitroguanidino)-1,2,4,5-tetrazine (BANTz), 2,2′-(carbonylamino)-1-binitroguanidine (CABNG), 2,2′-(malonylamino)-1-binitroguanidine (MABNG), 1-(formylamino)-2-nitroguanidine (FANG), and 1-(acetylamino)-2-nitro- guanidine (AANG), respectively. The synthesis routes for nitroguanidine derivatives are shown in Scheme 1, and the specific steps are as follows.

N-Methyl-N-nitroso-N′-nitroguanidine (MNNG) was prepared according to previously reported methods [17].

The synthesis of ANPTz/BANTz:

(3-(3,5-dimethylpyrazole)-6-hydrazino-1,2,4,5-tetrazine (DPHT) and 3,6-dihydrazino-1,2,4,5-tetrazine (DHT) were synthesized according to the literature method [21, 22].

MNNG (0.17 g, 1.1 mmol)/ (0.34 g, 2.2 mmol) were added to an aqueous solution (50 mL) of DPHT (0.206 g, 1 mmol)/DHT (0.142 g, 1 mmol) at room temperature. The mixture was stirred at room temperature for 18 h. Then, the precipitate was filtered off, washed with cold water, and dried to give ANPTz/BANTz.

ANPTz is red powder (50 %, 0.103 g). Elemental analysis calcd (%) for C$_8$H$_{11}$N$_{11}$O$_2$: C, 32.77; H, 3.78; N, 52.54; found: C, 32.23; H, 3.57; N, 52.24. FT-IR (KBr, υ/cm^{-1}): 3396(w), 3209(w), 2927(m), 1637(s), 1589(s), 1573(w), 1489(m), 1292(s), 1197(s), 1069(m), 939(m), 881(m), 807(s), 721(w), 571(m), 473(s), 415(m). ^{1}H NMR(DMSO-d_6): $\delta = 10.84$ (s, 1H, −NH−), 10.30 (s, 1H, −NH−), 8.76(s, 1H, −NH), 8.37 (s, 1H, −NH), 6.26 (s, 1H, −CH−), 2.46 (s, 3H, −CH$_3$), 2.24 (s, 3H, −CH$_3$) ppm. ^{13}C NMR (DMSO-d_6): $\delta = 162.41$ (s, 1 C, −C−N), 161.45 (s, 1 C, −C−NH), 158.51 (s, 1 C, −C−NH$_2$), 151.16 (s, 1 C, −C−CH$_3$), 141.93(s, 1 C, −C−CH$_3$), 109.57 (s, 1 C, −C−H), 13.52 (s, 1 C, −CH$_3$), 12.86 (s, 1 C, −CH$_3$) ppm. ^{14}N NMR(DMSO-d_6): $\delta = -12$(NO$_2$) ppm.

BANTz is orange powder (86 %, 0.27 g). Elemental analysis calcd (%) for C$_4$H$_8$N$_{14}$O$_4$: C, 15.19; H, 2.55; N, 62.02; found: C, 15.07; H, 2.48; N, 61.79. FT-IR (KBr, υ/cm^{-1}): 3375(w), 3211(w), 2987(m), 2901(m)1616(s), 1575(s), 1521(w), 1319(s), 1282(m), 1188(m), 1066(s), 1028(w), 945(s), 761(m), 569(w), 470(m). ^{1}H NMR (DMSO-d_6): $\delta = 10.10$ (s, 1H, −NH−), 9.95 (s, 1H, −NH−), 8.62 (s, 1H, −NH), 8.43(s, 1H, −NH) ppm. ^{13}C NMR (DMSO-d_6): $\delta = 167.37$ (s, 1 C, −C−NH), 161.51 (s, 1 C, −C−NH$_2$) ppm. ^{14}N NMR(DMSO-d_6): $\delta = -12$(NO$_2$)ppm.

The synthesis of FANG/CABNG/MABNG:

MNNG (0.17 g, 1.1 mmol)/ (0.34 g, 2.2 mmol)/ (0.34 g, 2.2 mmol) were added to an aqueous solution (50 mL) of formyl hydrazine (0.06 g, 1 mmol)/ carbon hydrazide (0.09 g, 1 mmol)/ propylene hydrazide (0.132 g, 1 mmol) at room temperature. The mixture was stirred at room tem-
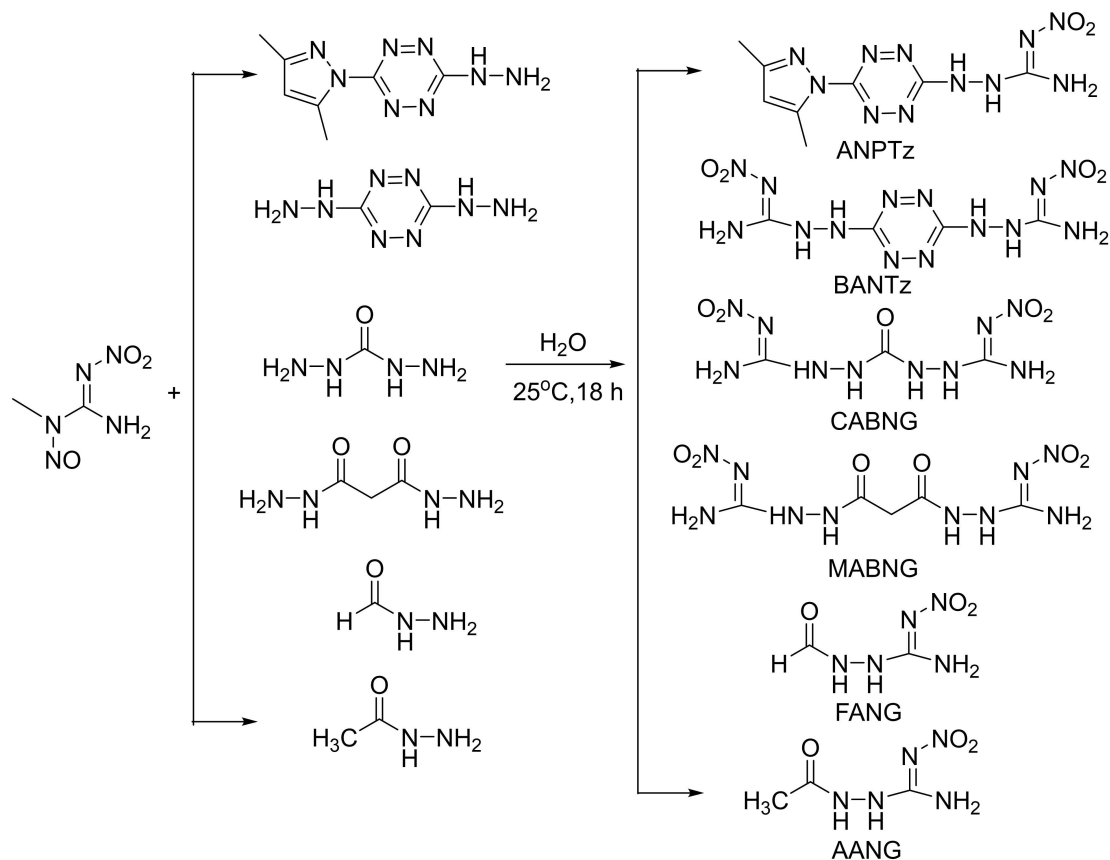
Scheme 1. The synthesis route of six compounds.

perature for 18 h. Then, the precipitate was filtered off, washed with cold water, and dried to give FANG/CABNG/MABNG.

FANG is white powder (82%, 0.12 g). Elemental analysis calcd (%) for $C_2H_5N_5O_3$: C, 16.33; H, 3.43; N, 47.61; found: C, 16.21; H, 3.17; N, 47.42. FT-IR (KBr, v/cm^{-1}): 3286(w), 3194 (w), 1693(w), 1616(m), 1566(w), 1504(w), 1419(w), 1315(s), 1225(m), 1111(s), 1057(w), 866(w), 762(s), 719(m), 604(m), 500(m). ^{1}H NMR (DMSO-d_6): $\delta = 10.01$(s, 1H, —NH—), 9.69 (s, 1H, —NH—), 8.58 (s, 1H, —NH), 8.28 (s, 1H, —NH), 8.04 (s, 1H, —CHO) ppm. ^{13}C NMR (DMSO-d_6): $\delta = 167.10$(s, 1 C, —C=O), 161.54(s, 1 C,—C=N) ppm. ^{14}N NMR(DMSO-d_6): $\delta = -12$(NO$_2$) ppm.

CABNG is white powder (69%, 0.18 g). Elemental analysis calced (%) for $C_3H_8N_{10}O_5$: C, 13.64; H, 3.05; N, 53.02; found: C, 13.24; H, 2.96; N, 52.97. FT-IR (KBr, v/cm^{-1}): 3385 (w), 3286(w), 2927(m), 3217(m), 3113(w), 1647(s), 1558(s), 1423(s), 1346(m), 1290(s), 1244(m), 1174(w), 1055(s), 771(w), 677(m), 561(w), 472(m). ^{1}H NMR (DMSO-d_6): $\delta = 9.61$(s, 1H, —NH—), 8.96(s, 1H, —NH—), 8.71(s, 1H, —NH), 8.17(s, 1H, —NH) ppm. ^{13}C NMR (DMSO-d_6): $\delta = 161.82$ (s, 1 C, —C—NH), 156.92 (s, 1 C, —C—NH$_2$) ppm. ^{14}N NMR(DMSO-d_6): $\delta = -12$(NO$_2$) ppm.

MABNG is white powder (75%, 0.23 g). Elemental analysis calcd (%) for $C_5H_{10}N_{10}O_6$: C, 19.61; H, 3.29; N, 45.74; found: C, 19.31; H, 3.02; N, 45.57. FT-IR (KBr, v/cm^{-1}): 3514 (m), 3387(w), 3207(w), 3101(m), 3008(w), 1716(s), 1678(m), 1622(s), 1585(s), 1520(s), 1313(w), 1265(m), 1170(s), 1024(m), 981(s), 789(s), 605(m). ^{1}H NMR (DMSO-d_6): $\delta = 10.24$ (s, 1H, —NH—), 9.80 (s, 1H, —NH—), 8.77 (s, 1H, —NH), 8.13 (s, 1H, —NH), 3.27 (s, 2H, —CH$_2$—) ppm. ^{13}C NMR (DMSO-d_6): $\delta = 175.21$ (s, 1 C, —C=O), 166.97 (s, 1 C, —C=N), 26.45 (s, 1 C, —CH$_2$—) ppm. ^{14}N NMR(DMSO-d_6): $\delta = -12$(NO$_2$)ppm.

The synthesis of AANG:

MNNG (0.17 g, 1.1 mmol) were added to deionized water (50 mL) dissolved with acetyl hydrazine (0.074 g, 1 mmol). The mixture was stirred at room temperature for 18 h. The resulting clear solution was cooled in an ice-water bath for 30 min, the white precipitate was filtered off, washed with cold water, and dried to give AANG.

AANG is white powder (74%, 0.12 g). Elemental analysis calcd (%) for $C_3H_7N_5O_3$: C, 22.36; H, 4.38; N, 43.47; found: C, 22.17; H, 4.21; N, 43.13. FT-IR (KBr, v/cm^{-1}): 3377(w), 3327 (w), 3180(w), 3072(m), 2933(w), 1674(w), 1626(w), 1568(s), 1504(m), 1415(s), 1367(w), 1296(w), 1265(s), 1087(m), 1033 (m), 989(m), 790(m), 734(w), 646(w), 579(w). ^{1}H NMR(DMSO-d_6): $\delta = 9.88$ (s, 1H, —NH—), 9.61 (s, 1H, —NH—), 8.62 (s, 1H, —NH), 8.21 (s, 1H, —NH), 1.87(s, 3H, —CH$_3$) ppm. ^{13}C NMR

(DMSO-d_6): $\delta = 169.81$ (s, 1 C, $-$C$=$O), 161.36 (s, 1 C, $-$C$=$N), 21.05 (s, 1 C, $-$CH$_3$) ppm. ^{14}N NMR(DMSO-d_6): $\delta = -12$(NO$_2$) ppm.

3 Results and Discussion

3.1 Crystal Structure

Fortunately, the single-crystal structures of ANPTz, CABNG·2H$_2$O, and FANG suitable for X-ray analyses were obtained by slow crystallization from the filtrate for several days and the basic crystal data and structural refinement details were summarized in Table 1.

ANPTz crystallizes in the triclinic space group P-1(Z$=$2) with a nitroguanidine group at the hydrazine group of 3-(3,5-dimethylpyrazole)-6-hydrazino-1,2,4,5-tetrazine (DPHT), and two intramolecular hydrogen bonds (N(9)$-$H(9)…N(11) and N(9)$-$H(9)…O(1)) are formed at the amino group of guanidine (Figure 1a). The hydrogen bonds are connected to adjacent atoms to form a five-membered ring and a six-

membered ring, respectively. From the torsional angle data of ANPTz (N11$-$N10$-$C8$-$N8 (174.5 (5)), N11$-$N10$-$C8$-$N9 ($-$7.9 (9)), Table S1), it is known that the atoms on the nitroguanidine are all on the same plane, while the tetrazine ring located between the nitroguanidine group and the pyrazole group is twisted (N7$-$N8$-$C8$-$N9 ($-$5.3 (9)) and C2$-$N1$-$C6$-$N3 (174.5 (6))), which make the coplanarity of whole molecule is poor.

Due to the conjugation of the tetrazine ring, the bond length of C$-$N in tetrazine ring is between 1.31 Å and 1.37 Å, and the bond length tends to be average, which is beneficial to improving the stability of the molecule. The bond angle of pyrazole ring, N2$-$N1$-$C2 (112.9(5)), N1$-$N2$-$C4 (103.6(5)), C2$-$C3$-$C4 (106.6 (6)), N1$-$C2$-$C3 (104.4(6)) and N2$-$C4$-$C3 (112.4 (6)), did not change much before and after the formation of the new compound, indicating that the structure of the pyrazole ring is relatively stable.

There are two intramolecular hydrogen bonds and five intermolecular hydrogen bonds in the ANPTz molecule (Table S2). Under these hydrogen bonds, an individual mole-

Table 1. Crystal data and structure refinement parameters for ANPTz, CABNG·2H$_2$O and FANG.

|	ANPTz	CABNG·2H$_2$O	FANG
Empirical formula	C$_8$H$_{11}$N$_{11}$O$_2$	C$_3$H$_{12}$N$_{10}$O$_7$	C$_2$H$_5$N$_5$O$_3$
Formula mass (g·mol^{-1})	293.28	300.23	147.11
Crystal system	Triclinic	Orthorhombic	Monoclinic
Temperature (K)	296	296	296
Space group	*P*-1	*Pnma*	*P*2$_1$/*c*
a (Å)	7.867(4)	19. 395(7)	4.279(3)
b (Å)	8.873(5)	14.678(5)	16.116(11)
c (Å)	9.501(5)	4.4695(15)	8.233(5)
α (°)	79.493(11)	90	90
β (°)	80.385(11)	90	97.174(9)
γ (°)	86.021(10)	90	90
V (Å^3)	642.4(6)	1272.4(8)	563.3(6)
Z	2	4	4
D_{calc} (g·cm^{-3})	1.516	1.567	1.735
θ range (°)	2.3-25.0	2.1-25.6	2.5-25.0
F (000)	304	624	304
Independent reflections (R$_{int}$)	0.091	0.147	0.107
Goodness-of-fit on F^2	1.132	1.251	1.190
Final R_1, wR_2 [I$>$2σ(I)]	0.0723, 0.1725	0.0504, 0.1000	0.0489, 0.0943
CCDC	2073383	2072493	2073381
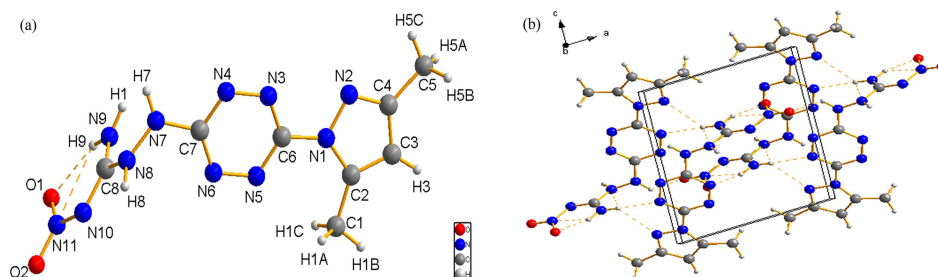
Figure 1. Molecular structure (a) and Hydrogen bonds (b) of ANPTz.

cule is connected to form a network structure, as shown in Figure 1b (along the *b*-axis), and then through five intermolecular hydrogen bonds: N(9)—H(1)…N(3), N(8)—H(8)…N-(10), N(8)—H(8)…O(2), N(9)—H(1)…N(2) and N(7)—H(7)…O(2) bridge each other to form three-dimensional structure (Figure S1).

The compound of CABNG·2H$_2$O belongs to orthorhombic system and the space group is *Pnma*. There are two nitroguanidine groups in CABNG·2H$_2$O molecular structure, and the whole molecular is symmetrical in the plane of two water molecules. The intramolecular hydrogen bond (N3—H1···O2 and O5—H5···O4) formed by the O and N atoms in nitroguanidine make the compound form two six-member ring structures at both ends. The other intramolecular hydrogen bond is formed by the O atoms of the two water molecules. (Figure 2a). From the data of torsion angle (Table S3), the atoms on both sides of the nitroguanidine groups are located on their respective planes and present "W" structure centered on C1 atom. The bond lengths of C—N and N—N bonds (C1—N1 (1.365 Å), C2—N2 (1.333 Å), C2=N4 (1.352 Å), N1—N2 (1.378 Å), and N4—N5 (1.342 Å) on the main chain are very close, which may be due to electron delocalization that make the bond lengths tend to average and the bond angles tend to 120°.

There are two intramolecular hydrogen bonds and six intermolecular hydrogen bonds, as shown in table S4. The CABNG·2H$_2$O molecule form a one-dimensional chain structure through hydrogen bond of N2—H2···N4. Because of the "W" structure of molecular itself, the whole chain structure extends in waves. The 2D planar structure is then formed
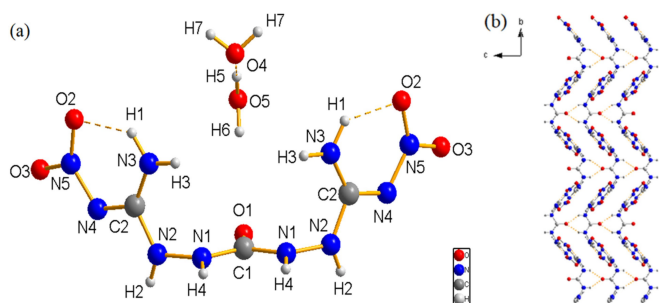
by the interaction of hydrogen bonds (N1—H4···O1) (Figure 2b). Finally, the 2D layer structure connected through three hydrogen bonds (N3—H3···O5, N3—H1···O2, O4—H7···O3 and N2—H2···O3) and van der Waals forces to form a 3D structure (Figure S2a). The existence of hydrogen bonds, such as N2—H2···N4, and N1—H4···O1, makes each molecular interconnected to form a tight regular network structure (Figure S2b).

Similar to CABNG·2H$_2$O, the molecular of FANG is also chain structure and a nitroguanidine group is attached to the hydrazine group of formyl hydrazine (Figure 3a). The N atom on the amino group forms intramolecular hydrogen bonds with the O atom of the nitro group and the N atom on the main chain, respectively (N3—H3B…O2 and N3—H3A…N1). According to the torsion angle data (Table S5), the distortion occurs at the junction of hydrazine and nitroguanidine, and amino and nitroguanidine, which makes the whole molecule in poor coplanar.

The 2D planar structure (Figure 3b) is formed with the interaction of two intermolecular hydrogen bonds (N3—H3A···O1 and N1—H1···O3) (Table S6). The schematic diagram of hydrogen bonding along the *a* axis is shown in Figure S3a, the atoms of N3 and N1 are used as hydrogen bond donors to form a 17-member ring structure ($R_2^2(17)$) and a 14-member ring structure ($R_2^2(14)$) through the intermolecular hydrogen bonds of N3—H3A···O1 and N1—H1···O3. Furthermore, O3 atom act as hydrogen bond acceptor to form a stable 5-membered ring ($R_2^1(5)$) by two hydrogen bonds (N2—H2···O3 and N1—H1···O3). Owing to the interaction of intermolecular hydrogen bonds, the three-dimensional spatial structure is constituted between molecules (Figure S3b), and the different size rings are also benefit to enhance the stability of compound.

Figure 2. Molecular structure (a) and 2D structure(b) of CABNG·2H$_2$O.

3.2 Impact Sensitivity

Impact sensitivity refers to the degree of combustion or explosion of energetic compounds when subjected to a certain physical impact. To assure the safety of six nitroguanidine derivatives, the test of impact sensitivity (*IS*) was carried out using a standard BAM Fall hammer, and the result indicated that *IS* of all the compounds is good. AANG was found to be less impact sensitive than TNT (*IS* is 15 J), and the sensitivity of the others was close to that of RDX (*IS* is 7.4 J) (Table 2). Molecule packing and non-covalent bonding interactions have significant effects on the safety of energetic materials [23]. Layered stacking and hydrogen bonding interactions have been shown to play an important role in reducing mechanical sensitivity [24]. The impact sensitivity of FANG is acceptable, which could be explained by its structural features. As seen in Figure S3b, it is the interaction of these intermolecular hydrogen bonds that makes FANG crystals behave as layered stacking structures in 3D, thus buffering external stimuli and reducing sensitivity.

Figure 3. Molecular structure (a) and 2D structure(b) of FANG.

Table 2. The impact sensitivity of the synthesized compounds, TNT and RDX.

Compounds	ANPTz	BANTz	FANG	AANG	CABNG	MABNG	TNT	RDX
IS(J)	>7.45	>8.82	>7.84	>15.68	>6.86	>9.8	15	7.4

3.3 Thermal Analysis

It is of great significance to study the thermal decomposition behavior of energetic materials [25]. Differential scanning calorimetry (DSC) and thermogravimetry-derivative thermogravimetry (TG-DTG) were applied to study the thermal behavior of six compounds, and the curves of DSC and TG-DTG at heating rate of $10\,°C\,min^{-1}$ were shown in Figure 4. There is an endothermic peak at $64.10\,°C$ (the melting of free water) and an exothermic peak at $202.17\,°C$ (thermal decomposition) for compound MABNG, while, the others have only one exothermic process with exothermic peak temperature (T_p) of $211.03\,°C$ (ANPTz), $200.32\,°C$ (BANTz), $207.16\,°C$ (CABNG), $200.96\,°C$ (FANG), and $196.81\,°C$ (AANG), respectively. Except for the compound AANG $(T_p = 196.81\,°C)$, the thermal decomposition temperatures of the other compounds were above $200\,°C$, and ANPTz was the best one with T_p of $211.03\,°C$. From the curves of TG-DTG, the weight loss of several compounds in the exothermic stage are inferred to be the departure of pyrazole and nitroguanidine groups in compound ANPTz (73.76%, theoretical value is 72.70%), the breakage of two nitroguanidines groups (54.29%, 55.69% (theoretical value) for BANTz), the loss of the hydrazine and nitroguanidine for CABNG (31.19%, 33.34% for the theoretical value), and the fracture of propyl hydrazide, formyl hydrazide, and acetyl groups in compounds of MABNG, FANG, and AANG (45.28%, 39.21%, and 46.04%). Furthermore, the mass loss of 9.21% occurring at $49\sim98\,°C$ for MABNG may be due to the simultaneous melting and decomposition of two free water molecules, which is consistent with the theoretical one (10.52%).

Gaseous products generated after thermal decomposition for the title compounds were also detected by DSC-TG-FTIR-MS coupling technique. From figure S4a - S7b, four gases are produced in the thermal decomposition process for ANPTz, BANTz, MABNG, and AANG: HCN($m/z = 27$, $v = 732\,cm^{-1}$/ $m/z = 27$, $v = 714\,cm^{-1}$/$m/z = 27$, $v = 672\,cm^{-1}$/$m/z = 27$, $v = 682\,cm^{-1}$), NO_2 ($m/z = 30$, $v = 1678\,cm^{-1}$/$m/z = 30$, $v = 1626\,cm^{-1}$/$m/z = 30$, $v = 1736\,cm^{-1}$/$m/z = 30$, $v = 1775\,cm^{-1}$), H_2O ($m/z = 17$, $m/z = 18$, $v = 3359\,cm^{-1}$, $v = 3267\,cm^{-1}$/$m/z = 17$, $m/z = 18$, $v = 3333\,cm^{-1}$, $v = 3275\,cm^{-1}$/$m/z = 17$, $m/z = 18$, $v = 3376\,cm^{-1}$, $v = 3269\,cm^{-1}$/$m/z = 17$, $m/z = 18$, $v = 3376\,cm^{-1}$, $v = 3269\,cm^{-1}$), CO_2 ($m/z = 44$, $v = 2107\,cm^{-1}$, $v = 2262\,cm^{-1}$/$m/z = 44$, $v = 2309\,cm^{-1}$, $v = 2242\,cm^{-1}$/$m/z = 44$, $v = 2248\,cm^{-1}$, $v = 2379\,cm^{-1}$/$m/z = 44$, $v = 2269\,cm^{-1}$, $v = 2345\,cm^{-1}$). It means that the groups of pyrazole and nitroguanidine, two nitroguanidines, malonic dihydrazide and acetyl hydrazide are ground fractured respectively [26]. Besides, the gas produce of FANG include not only H_2O ($m/z = 17$, $m/z = 18$, $v = 3376\,cm^{-1}$, $v = 3269\,cm^{-1}$), HCN ($m/z = 26$, $m/z = 27$, $v = 661\,cm^{-1}$), CO_2 ($m/z = 44$, $v = 2242\,cm^{-1}$, $v = 2311\,cm^{-1}$), and NO_2 ($m/z = 30$, $v = 1735\,cm^{-1}$), but also NH_3 ($m/z = 16$, $m/z = 17$, $v = 1262\,cm^{-1}$, $v = 1131\,cm^{-1}$), which may be caused by the fracture of formyl hydrazine group (Figure S8a and S8b). Furthermore, according to the IR and
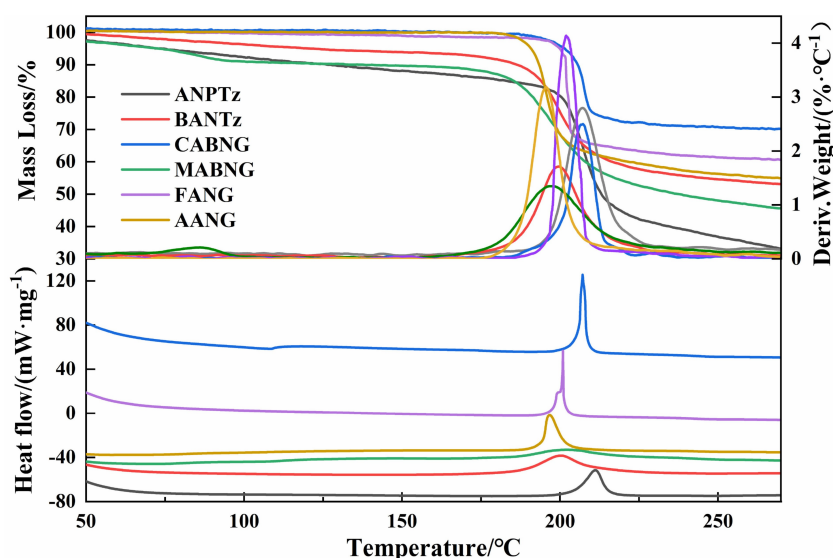
Figure 4. TG-DTG and DSC curves of six compounds.

mass spectrometry, the more gas types are produced for CABNG, and they are NH_3 ($m/z = 15$, $m/z = 16$, $m/z = 17$, $v = 930$ cm^{-1}, $v = 964$ cm^{-1}), H_2O ($m/z = 18$, $v = 3376$ cm^{-1}, $v = 3269$ cm^{-1}), HCN ($m/z = 27$, $v = 714$ cm^{-1}), HCNO ($m/z = 43$, $v = 2280$ cm^{-1}), NO_2 ($m/z = 30$, $v = 1630$ cm^{-1}) and CO_2 ($m/z = 44$, $v = 2350$ cm^{-1}, $v = 2210$ cm^{-1}), which is due to the pyrolysis of carbonyl hydrazine (Figure S9a and S9b).

3.4 Non-Isothermal Kinetics Analysis

To obtain the apparent activation energies (E_a) of the main exothermic decomposition reaction for six compounds, both Kissinger's method [27] and Ozawa's method [28] (Equations (1) and (2)) were employed.

Differential method, Kissinger equation:

$$\frac{d \ln \frac{\beta}{T_p^2}}{d \frac{1}{T_p}} = -\frac{E}{R} \tag{1}$$

Integral method, Ozawa equation:

$$lg\, \beta + \frac{0.4567E}{RT} = C \tag{2}$$

Where, β is the linear heating rate (°C·min); T_p is the peak temperature (°C); R is the gas constant (8.314 J·mol^{-1}·K^{-1}), E is the apparent activation energy (kJ·mol^{-1}) and C is a constant for a certain compound.

According to the exothermic peak temperature determined at four different heating rates of 5, 10, 15, and 20 °C·min^{-1}, the kinetic parameters of six compounds are listed in Table 3. The apparent activation energies based on Ozawa equation are calculated using both the extrapolated onset temperatures (T_e) and the peak temperatures (T_p) from DSC analyses. The apparent activation energies obtained from Kissinger equation are labeled as E_k. The values of E_{po} and E_{pk} for each compound are close to each other. However, the value of E_{eo} deviates from E_{po} value significantly, indicating the thermal decomposition mechanism of initial stage is different from that the rapid decomposition stage. No matter which equation and data are used to calculate, the apparent activation energy of ANPTz is the highest, which also indicates that it has the best thermodynamic stability among the six compounds.

It is of great significance to analyze and evaluate the thermal safety of energetic compounds to reduce the risks during production, storage, and transportation [29,30]. The commonly used parameters for thermal safety assessment are self-accelerating decomposition temperature (T_{SADT}) and thermal explosion critical temperature (T_b). T_{SADT} is determined based on Equations (3) and (4), which is calculated from T_e (onset temperature) at different heating rates (β) when β tend to 0. T_b is obtained by substituting E_{po} and T_{p0} into Equation (5).

Table 3. The various heating rates kinetic parameters of six compounds.

Compd	β	T_e	T_p	E_{pk}	r_k	E_{po}	r_{po}	E_{eo}	r_{eo}	T_{SADT}	T_b
ANPTz	5	198.15	206.21								
	10	204.65	211.03	274.03	0.9997	268.24	0.9997	168.61	0.9953	194.12	208.63
	15	210.47	213.78								
	20	212.39	215.81								
BANTz	5	179.94	192.56								
	10	187.23	200.32	157.40	0.9990	157.16	0.9991	136.94	0.9976	182.52	207.54
	15	192.78	204.40								
	20	196.98	208.41								
FANG	5	194.96	195.71								
	10	199.15	200.96	177.02	0.9997	175.85	0.9997	175.99	0.9953	198.68	209.97
	15	205.46	206.26								
	20	208.10	208.93								
AANG	5	189.17	190.96								
	10	194.48	196.81	214.16	0.9997	211.08	0.9997	226.53	0.9999	180.04	188.35
	15	197.61	199.89								
	20	199.71	202.50								
CABNG	5	197.64	199.00								
	10	206.44	207.16	202.79	0.9772	200.39	0.9788	186.81	0.9764	176.80	187.32
	15	208.78	209.41								
	20	210.24	210.87								
MABNG	5	180.33	194.58								
	10	185.82	202.17	173.68	0.9953	172.66	0.9957	194.47	0.9991	173.61	184.29
	15	189.82	205.49								
	20	192.07	209.09								

$$T_{e\ or\ p} = T_{e0\ or\ p0} + a\beta_i + b\beta_i^2 + c\beta_i^3, i = 1 \sim 4 \tag{3}$$

$$T_{SADT} = T_{e0} \tag{4}$$

$$T_b = \frac{E_O - \sqrt{E_O^2 - 4E_ORT_{p0}}}{2R} \tag{5}$$

where a, b and c are coefficients.

Based on the result of calculation, the thermal safety of the compounds from high to low is FANG > ANPTz > BANTz > AANG > CABNG > MABNG. The thermal stability of four nitroguanidine derivatives with chain structure decreases with the elongation of the molecular skeleton and the increase of nitroguanidine.

3.5 Energy Performance

Whether the oxygen contained in CHON energetic compounds can be completely oxidized has a certain guiding role in studying the detonation properties such as detonation heat, detonation velocity, and detonation capacity of energetic compounds, which can be evaluated by oxygen balance (OB) [31].

Based on CO_2, the compounds exhibited negative OB values ranging between −36.34% (CABNG) and −106.39% (ANPTz), and the oxygen balance of CABNG (−36.34%) and FANG (−38.07%) is higher than that of TNT (−73.97%) but lower than that of RDX (−21.61%).

The detonation velocity(D) and detonation pressure(P) of energetic material are important parameters to measure the detonation performance [32]. Nitrogen equivalent formula (NE equation) is one of the empirical formulas for calculating compounds D and P, which has been widely used for its convenience, accuracy, and rapidity [33], and the equations are listed below.

$$\sum N = 100 \sum x_i N_i / M \tag{6}$$

$$D = (690 + 1160\rho_0) \sum N \tag{7}$$

$$P = 1.092 \left(\rho_0 \sum N\right)^2 - 0.574 \tag{8}$$

In the equations, $\sum N$, ρ_0, N_i and x_i are the nitrogen equivalent of the substance, the density of the compound, the nitrogen equivalent coefficient of the detonation product, and the number of molecules formed by the reaction of the unit reactants, respectively.

Density (ρ) is a critical physical parameter for energetic materials and has directly affect on detonation performance. The values of detonation velocity and pressure for ANPTz, CABNG, and FANG were calculated according to their crystal density, while the values of other compounds were calculated based on the theoretical density values obtained by Rice's formula [34]. The crystal density prediction formula is shown in Equation 9.

$$\rho = \frac{M}{V_m} \tag{9}$$

Where M is the molecular mass in $g \cdot mol^{-1}$, V_m is the volume of the inside of the electron density contour of 0.001 $e \cdot bohr^{-3}$. The density values of the six compounds were calculated using B3PW91/6-31G (d, p) and the results were shown in Table 4. It can be seen that the experimental values for ANPTz and FANG are in good agreement with the calculated one, and the errors are 0.033 and 0.031 $g \cdot cm^{-3}$, respectively. Since CABNG crystal structure contains two water molecules, its density decreases significantly, and M/V_m is much less than 1.782 $g \cdot cm^{-3}$. Although the crystal structures are not obtained for the other three compounds, the density and detonation parameters (D and P) calculated by M/V_m are reliable. The detonation velocities (the theoretical value) of the synthesized energetic compounds are between 7341 $m \cdot s^{-1}$ to 8665 $m \cdot s^{-1}$, and the detonation pressures (the theoretical value) range from 22.41 GPa to 33.52 GPa, which are superior to the traditional explosive TNT (D = 6881 $m \cdot s^{-1}$, P = 19.50 GPa) but weaker than the RDX values. Among these compounds, CABNG has the best detonation performance at the theoretical level (D = 8558 $m \cdot s^{-1}$, P = 32.84 GPa) and its value is close to that of RDX (D = 8748 $m \cdot s^{-1}$, P = 34.9 GPa), which may be due to its best oxygen balance. Because of the high density and good oxygen balance, the compound BANTz also has high theoretical detonation performance. However, from the crystal data, FANG had the best detonation performance (D = 8551 $m \cdot s^{-1}$, P = 32.33 GPa) of these compounds, and slightly lower than that of RDX.

Table 4. The detonation performance of six compounds was compared with that of TNT and RDX.

Compound	OB (%)	ΣN	ρ (g·cm^{-3})	D (m·s^{-1})	P (GPa)
ANPTz	−106.39	2.999	1.516[a]	7343[a]	22.00[a]
			1.549[b]	7458[b]	22.99[b]
BANTz	−40.48	3.086	1.741[b]	8362[b]	30.95[b]
CABNG	−36.34	3.104	1.567[a]	7784[a]	25.26[a]
			1.782[b]	8558[b]	32.84[b]
MABNG	−47.03	2.965	1.698[b]	7886[b]	27.10[b]
FANG	−38.07	3.164	1.735[a]	8551[a]	32.33[a]
			1.766[b]	8665[b]	33.52[b]
AANG	−64.54	2.926	1.568[b]	7341[b]	22.41[b]
TNT [35, 36]	−73.97	–	1.650	6881	19.50
RDX [37]	−21.61	–	1.820	8748	34.90

[a] Single crystal density measured (23 °C); [b] Density calculated by M/V_m.

3.6 Catalytic Property

The thermal decomposition catalytic activity of six compounds to RDX was studied by DSC method at heating rate (β) of 10 °C·min^{-1}. The inert atmosphere is nitrogen and its flow rate is 20 mL·min^{-1}. After mixing the title compound with RDX (1:4, g:g), it was placed in an aluminum crucible for testing.

As shown in Figure 5, pure RDX had an exothermic process with a peak temperature of 240.60 °C, and the peak temperatures of ANPTz, BANTz, CABNG, MABNG, FANG, and AANG were 211.03 °C, 200.32 °C, 207.16 °C, 202.17 °C, 200.96 °C, and 196.81 °C, respectively. Unlike other compounds, the decomposition temperature AANG compounds increased (226.48 °C), while those of other compounds decreased to 195.97 °C, 198.34 °C, 204.78 °C, 197.54 °C, and 199.20 °C, respectively. Furthermore, compounds of ANPTz, BANTz, CABNG, FANG reduced the decomposition temperature of RDX to 233.34 °C, 235.66 °C, 232.36 °C, 232.29 °C, respectively. In other words, the thermal decomposition temperature of RDX was decreased by 7.26 °C, 4.94 °C, 8.24 °C, 8.31 °C, respectively. Unfortunately, the peak temperature of MABNG/RDX (241.56 °C) and AANG/RDX (239.58 °C) were very close to that of pure RDX (240.60 °C), indicating that they had almost no catalysis to RDX. The results showed that the other compounds except for MABNG and AANG had a certain catalytic effect on the thermal decomposition of RDX, among which FANG had the most significant catalytic thermal decomposition effect on RDX.
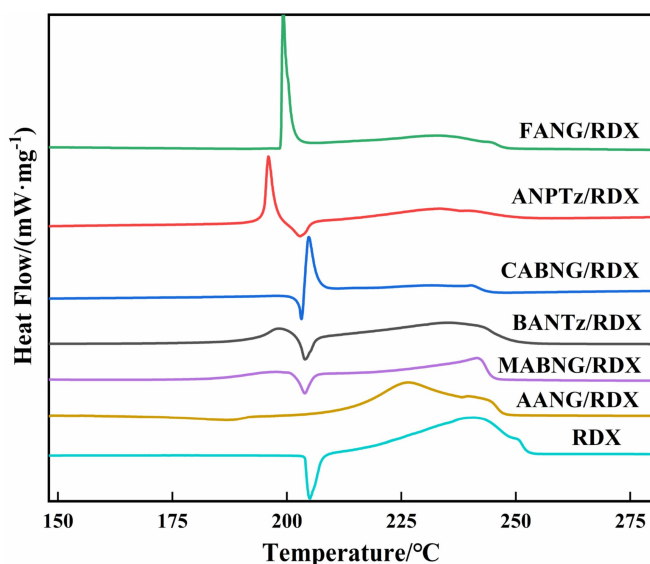
4 Conclusion

In summary, six nitroguanidine derivatives were synthesized and characterized by EA, FT-IR, and NMR, and the single-crystal structure of ANPTz, CABNG, and FANG was further determined by XRD. The thermal decomposition behavior was studied by the DSC-TG-FTIR-MS coupling technique, and the result indicated that ANPTz had the best thermal stability ($E_{pk} = 274.03$ kJ·mol^{-1}, $T_d = 211.03$ °C), and the gaseous product of HCN, CO$_2$, H$_2$O, and NO$_2$ was released during the decomposition process for six compounds. Besides, the research results showed that FANG had the highest thermal safety ($T_{SADT} = 198.68$ °C, $T_b = 209.97$ °C), acceptable sensitivity ($IS = 7.84$ J), excellent explosive properties ($D = 8551$ m·s^{-1}, $P = 32.33$ GPa), and had a significant catalytic effect on the thermal decomposition of RDX (the thermal decomposition peak temperature decreased to 232.29 °C), which can be used as a potentially applicable energetic material.

Data Availability Statement

The data that supports the findings of this study are available in the supplementary material of this article.

References

[1] Z. Xu, H. W. Yang, G. B. Cheng, Studies on the synthesis and properties of polynitro compounds based on esteryl backbones, *New J. Chem.* **2016**, *40*, 9936–9944.

[2] Y.-H. Joo, B. Twamley, J. M. Shreeve, Carbonyl and oxalyl bridged bis(1,5-diaminotetrazole)-based energetic salts, *Chem. Eur. J.* **2009**, *15*, 9097–9104.

[3] Y.-H. Joo, B. Twamley, S. Garg, J. M. Shreeve, Energetic nitrogen-rich derivatives of 1,5-diaminotetrazole, *Angew. Chem.* **2008**, *120*, 6332–6335; *Angew. Chem. Int. Ed.* **2008**, *47*, 6236–6239.

[4] Y.-H. Joo, B. Twamley, S. Garg, J. M. Shreeve, Energetic nitrogen-rich derivatives of 1,5-diaminotetrazole, *Angew. Chem. Int. Ed.* **2008**, *47*, 6236–6239; *Angew. Chem.* **2008**, *120*, 6332–6335.

[5] H. Xue, H. X. Gao, B. Twamley, J. M. Shreeve, Energetic salts of 3-nitro-1,2,4-triazole-5-one, 5-nitroaminotetrazole, and other nitro-substituted azoles, *Chem. Mater.* **2007**, *19*, 1731–1739.

[6] V. Thottempudi, J. M. Shreeve, Synthesis and promising properties of a new family of high-density energetic salts of 5-nitro-3-trinitromethyl-1H-1,2,4-tri- azole and 5,5' bis(trinitromethyl)-3,3'-azo-1H-1,2,4-triazole, *J. Am. Chem. Soc.* **2011**, *133*, 19982–19992.

Figure 5. DSC curves of different compounds mixed with RDX.

[7] T. T. Vo, J. H. Zhang, D. A. Parrish, B. Twamley, J. M. Shreeve, New Roles for 1,1-Diamino-2,2-dinitroethene (FOX-7): Halogenated FOX-7 and Azo-bis(diahaloFOX) as Energetic Materials and Oxidizers, *J. Am. Chem. Soc.* **2013**, *135*, 11787–11790.

[8] O. Bolton, L. R. Simke, P. F. Pagoria, A. J. Matzger, High power explosive with good Sensitivity: A 2:1 Cocrystal of CL-20:HMX, *Cryst. Growth Des.* **2012**, *12*, 4311–4314.

[9] Z. Yang, Y. H. He, Pyrolysis of Octanitrocubane via molecular dynamics simulations, *Acta Phys. -Chim. Sin.* **2016**, *32*, 921–928.

[10] X. Li, S. S. Chen, X. Wang, F. Q. Shang, W. B. Dong, Z. Y. Yu, Y. H. Yu, H. M. Zou, S. H. Jin, Y. Chen, Effect of polymer binders on safety and detonation properties of ε-CL-20-based pressed-polymer-bonded explosives, *Mater. Express* **2017**, *7*, 209–215.

[11] L. M. He, Z. L. Xiao, D. Q. Jing, F. Y. Dong, Synthesis, properties and applications of ammonium dinitramide, *Chin. J. Energet. Mater.* **2003**, *11*, 170–173.

[12] N. V. Latypov, M. Johansson, L. N. Wahlström, S. Ek, C. Eldsäter, P. Goede, Synthesis and characterization of 1,2-dinitroguanidine (DNG and its derivatives), *Cent. Eur. J. Energ. Mater.* **2007**, *4*, 3–16.

[13] N. Fischer, T. M. Klapötke, J. Stierstorfer, 1-Amino-3-nitroguanidine (ANQ) in high-performance ionic energetic materials, *Z. Naturforsch.* **2012**, *67b*, 573–588.

[14] T. Wei, W. H. Zhu, X. W. Zhang, Y. F. Li, H. M. Xiao, Molecular design of 1,2,4,5-tetrazine-based high-energy density materials, *J. Phys. Chem. A* **2009**, *113*, 9404–9412.

[15] P. F. Pagoria, G. S. Lee, A. R. Mitchell, R. D. Schmidt, A review of energetic materials synthesis, *Thermochim. Acta* **2002**, *384*, 187–204.

[16] Z. C. Feng, X. G. Guan, K. Z. Xu, L. J. Zhai, F. Q. Zhao, Three new energetic compounds based on 1-amino-2-nitroguanidine (ANQ): synthesis, crystal structure and properties, *J. Mol. Struct.* **2018**, *1166*, 369–376.

[17] Q. H. Zhang, C. L. He, P. Yin, J. M. Shreeve, Insensitive nitrogen-rich materials incorporating the nitroguanidyl functionality, *Chem. Asian J.* **2014**, *9*, 212–217.

[18] Z. Xu, G. B. Cheng, H. W. Yang, X. H. Ju, P. Yin, J. H. Zhang, J. M. Shreeve, A facile and versatile synthesis of energetic furazan-functionalized 5-nitroimino-1,2,4-triazoles, *Angew. Chem. Int. Ed.* **2017**, *56*, 5877–5881.

[19] O. V. Dolomanov, L. J. Bourhis, R. J. Gildea, J. A. K. Howard, H. Puschmann, OLEX2: a complete structure solution, refinement and analysis program, *J. Appl. Crystallogr.* **2009**, *42*, 339–341.

[20] G. M. Sheldrick, Crystal structure refinement with SHELXL, *Acta Crystallogr. Sect. C* **2015**, *C71*, 3–8.

[21] X. Chen, C. Zhang, Y. Bai, Z. Q. Guo, Y. R. Yao, J. R. Song, H. X. Ma, Synthesis, crystal structure and thermal properties of an unsymmetrical 1,2,4,5-tetrazine energetic derivative, *Acta Crystallogr. Sect. C* **2018**, *74*, 666–672.

[22] K. Z. Xu, F. Q. Zhao, Y. H. Ren, H. X. Ma, J. R. Song, R. Z. Hu, Thermal behavior, specific heat capacity and adiabatic time-to-explosion of 3,6-dihydrazino-1,2,4,5-tetrazine, *Acta Phys. -Chim. Sin.* **2009**, *25*, 309–313.

[23] J. S. Li, Further study on the stine method to calculate the detonation velocity of energetic materials, *Chin. J. Explos. Propellants* **1996**, *1*, 43–46.

[24] Y. Ma, A. B. Zhang, C. H. Zhang, D. J. Jiang, Y. Q. Zhu, C. Y. Zhang, Crystal packing of low-sensitivity and high-energy explosives, *Cryst. Growth Des.* **2014**, *14*, 4703–4713.

[25] T. B. Brill, K. J. James, Kinetics and mechanisms of thermal decomposition of nitroaromatic explosives, *Chem. Rev.* **1993**, *93*, 2667–2692.

[26] X. Ma, X. H. Wang, F. Shang, Z. M. Ding, X. J. Hang, X. Zhang, S. H. Wei, K. Z. Xu, J. Huang, A study of two metal energetic complexes based on 4-amino-3-(5-tetrazolate)-furazan: synthesis, crystal structure, thermal behaviors and energetic performance, *J. Anal. Appl. Pyrolysis.* **2019**, *142*, 104666.

[27] H. E. Kissinger, Reaction kinetics in differential thermal analysis, *Anal. Chem.* **1957**, 29, 1702–1706.

[28] T. Ozawa, A new method of analyzing thermogravimetric data, *Bull. Chem. Soc. Jpn.* **1965**, *38*, 1881–1886.

[29] J. Y. Lv, L. P. Chen, W. H. Chen, H. S. Gao, M. J. Peng, Kinetics analysis and self-accelerating decomposition temperature (SADT) of dicumyl peroxide, *Thermochim. Acta* **2013**, *571*, 60–63.

[30] Z. H. Mi, Y. G. Bi, Y. A. Feng, T. L. Zhang, Synthesis, structure, and characterization of 3,4′-bis-1H-1,2,4-triazolium picrate salt: a new high-energry density material, *Z. Anorg. Allg. Chem.* **2016**, *642*, 317–322.

[31] D. D. Wang, G. Y. He, H. Q. Chen, Prediction for the detonation velocity of the nitrogen-rich energetic compounds based on quantum chemistry, *Russ. J. Phys. Chem. A* **2014**, *88*, 2363–2369.

[32] Y. X. Guo, H. S. Zhang, Nitrogen equivalent and modified nitrogen equivalent equations for predicting detonation parameter of explosives-prediction of detonation velocity of explosives, *Explos. Shock Waves* **1983**, *3*, 56–66.

[33] B. Yan, H. Y. Li, H. X. Ma, J. R. Song, F. Q. Zhao, N. N. Zhao, R. Z. Hu, Thermodynamic properties and detonation characterization of 3,3-dinitroazetidinium hydrochloride, *J. Chem. Eng. Data* **2013**, *58*, 3033–3038.

[34] B. M. Rice, J. J. Hare, E. F. C. Byrd, Accurate predictions of crystal densities using quantum mechanical molecular volumes, *J. Phys. Chem. A* **2007**, 111, 10874–10879.

[35] Y. Q. Zhang, Y. Guo, Y.-H. Joo, D. A. Parrish, J. M. Shreeve, 3,4,5-trinitropyrazole-based energetic salts, *Chem. Eur. J.* **2010**, *16*, 10778–10784.

[36] X. Y. Liu, Q. Yang, Z. Y. Su, S. P. Chen, G. Xie, Q. Wei, S. L. Gao, 3D high-energy-density and low sensitivity materials: synthesis, structure and physicochemical properties of an azide–Cu(ii) complex with 3,5-dinitrobenzoic acid, *RSC Adv.* **2014**, *4*, 16087–16093.

[37] R. Meyer, J. Köhler, A. Homburg, Explosives. Sixth Edition, Wiley VCH Verlag GmbH & Co. KGaA, Weinheim, **2007**, p. 208.